



## Article

# The Influence of Backfill on the Driving Energy Intensity and Axial Load Resistance of Piles with Shaft Widening: Modeling Research

Bekbasarov Isabai <sup>1</sup>, Atenov Yerlan <sup>1,\*</sup>  and Shanshabayev Nurzhan <sup>2</sup> <sup>1</sup> Geotechnical Testing Laboratory, Dulaty University, 60, Tole bi, Taraz 080000, Kazakhstan<sup>2</sup> Department of Construction and Production of Materials, Institute of Water Management and Environmental Engineering, Campus 6.2, Dulaty University, 28, Satpayev, Taraz 080000, Kazakhstan

\* Correspondence: yer\_at@mail.ru

**Abstract:** This article is dedicated to addressing the current challenge of augmenting the load-bearing capability of pile foundations. This predicament is most effectively addressed by employing piles with unconventional geometries along with atypical methodologies for installing these foundation piles. The primary objective of the research was to examine the impact of various fill materials (including both soil and rigid substances) on the energy consumption during pile driving and the resistance to static loads by piles with multiple shaft expansions. The findings derived from model-based investigations demonstrate that the load-bearing capacity of piles with shaft expansions installed with bulk material filling surpassed that of conventional piles (prismatic and pyramidal) by a factor ranging from 1.5 to 4.6. Furthermore, the research outcomes also indicated greater energy consumption (1.14–1.66 times) and enhanced load-bearing capacity (1.15–1.68 times) for piles with shaft expansions driven with backfill in comparison to piles installed without backfill. It is noteworthy that the type of backfill material significantly influenced the energy consumption during pile driving and their stability under axial static loads. The correlation relationships can be applied to approximate projection of the energy-related and structural parameters of piles with shaft expansions embedded with the addition of bulk materials.

**Keywords:** driven pile; pile with extensions; pile driving; backfilling of rigid material; static tests; deformation; axial load; resistance



**Citation:** Isabai, B.; Yerlan, A.; Nurzhan, S. The Influence of Backfill on the Driving Energy Intensity and Axial Load Resistance of Piles with Shaft Widening: Modeling Research. *Buildings* **2023**, *13*, 3097. <https://doi.org/10.3390/buildings13123097>

Academic Editor: Xiaoqiang Gu

Received: 30 October 2023

Revised: 4 December 2023

Accepted: 7 December 2023

Published: 13 December 2023



**Copyright:** © 2023 by the authors. Licensee MDPI, Basel, Switzerland. This article is an open access article distributed under the terms and conditions of the Creative Commons Attribution (CC BY) license (<https://creativecommons.org/licenses/by/4.0/>).

## 1. Introduction

Enhancing the load-bearing capacity of foundations, including pile foundations, constitutes a paramount concern in foundation engineering, especially when dealing with construction in soft soil conditions. The primary motivations behind its implementation include augmenting the foundation's load-bearing capacity in response to activities such as reconstruction, redevelopment, and the addition of floors to the building. This is essential for addressing the uneven distribution of loads on structural elements and mitigating dynamic effects, such as vibrations. Earthworks associated with construction activities, including the laying of utilities, further underscore the need for such measures.

Enhancing the bearing capacity of foundations not only prolongs the service life of buildings and structures but also achieves structural integrity and operational safety by fortifying foundations and stabilizing soils. This approach yields cost savings, as it obviates the necessity for new construction, opting instead for reinforcement measures.

One approach to address this challenge is the development and utilization of unconventional pile shaft shapes. Such variations encompass piles with shaft widening, thickening, profiled surfaces, and telescopic geometries, among others [1–5]. Owing to the distinctive characteristics of their shaft shapes, these piles demonstrate more efficient interaction with the surrounding soil, resulting in a significantly greater load resistance

than conventional prismatic or cylindrical piles. Field investigations [6] and numerical simulations [7] focusing on conical piles have revealed heightened stress concentration in the widening regions of the piles within the ground compared to their tips. This observation underscores the pivotal role of the widening sections in determining the load-bearing capacity of piles. Further research [8–11] indicates a 35–45% increase in the static load resistance of widened piles compared to their non-widened counterparts. In some numerical studies [12], this beneficial effect has been shown to reach as high as 68%.

Another equally effective strategy for augmenting the load-bearing capacity of foundations, including pile foundations, is the incorporation of loose, rigid materials (such as crushed stone, gravel, dry cement–sand mixtures, concrete mortar, etc.) during construction. This technique results in a 2.0–2.4-fold increase in foundation resistance [13]. It finds widespread application when establishing foundations in compacted excavations. The addition of rigid materials and their compaction at the base of the excavation serves as an effective means of compacting the surrounding soil, thereby increasing the foundation's load-bearing capacity [14,15]. This in turn leads to reduced excavation volume, decreased consumption of concrete and reinforcement materials, and cost savings in constructing buildings and structures.

Regarding pile foundations within geotechnical engineering, there exists a body of experience in using rigid-material backfills to enhance the load-bearing capacity of driven, bored, and cast-in-place piles.

The literature reveals the technology for fabricating driven hollow reinforced concrete piles with a circular cross-section and an open lower end [16,17]. To heighten the load-bearing capacity of such piles, it is recommended to partially fill their internal cavities with rigid materials and subsequently compact them with a punch into the ground beneath the pile's lower end. Crushed stone or dry concrete mixtures are proposed as suitable rigid materials. Consequently, the lower portion of the piles forms a compacted, broadened base comprising rigid materials and soil. The application of such hollow piles with backfilling and rigid-material compaction is advised for deployment in weak, waterlogged soils, where the most significant improvement in load-bearing capacity is anticipated.

The construction of tubular piles featuring crushed-stone widening in their lower sections is elucidated in [2,18]. To create the widening within the driven pile's cavity, portions of crushed stone are backfilled and compacted through the pile's cavity into the ground. Research has established that the dimensions of the widening in the lower part of the piles have a substantial influence on their static load resistance. Accordingly, the bearing capacity of a tubular pile with a widened, compacted crushed-stone portion having a diameter equivalent to 2.5 times the pile's diameter (denoted as 'd') is 1.7–2.45 times greater than that of similar piles lacking this feature. Researchers have further determined that the dimensions of the widening composed of rigid material are contingent on various factors, including the pile's diameter, the soil characteristics beneath the pile's lower end, the volume of compacted crushed-stone material, and its particle size distribution, among others [19].

Numerical modeling results elucidate the performance of bored-tied piles both with and without compacted crushed-stone widening in their lower sections [20]. It has been ascertained that the creation of crushed-stone widening in the lower part of the piles leads to additional soil compaction at the base, resulting in a 1.04–1.12-fold reduction in pile settlement.

The proposed PGP pile arrangement technology involves employing a spiral drill to bore a well to the specified depth [21]. Subsequently, an expanded head is formed at the bottom of the well, and a cement–soil core is established by injecting cement mortar into the well and blending it with the soil. The final step entails installing a PHC tubular pile filled entirely with the cement–soil mixture into the well. According to the proponents, this PGP pile construction method exhibits characteristics such as low noise levels during installation, high strength, an increased load-bearing capacity, and environmental friendliness as a foundation.

Model studies conducted on piles with irregular trunk widths have demonstrated notable efficacy attributed to their enhanced resistance to friction on the side surface [22]. These piles were created by injecting liquid concrete into a well within sandy soil, resulting in an irregular cylindrical shape along the length of the trunk (the diameter increase ranged from 1.06 to 1.34 times). Testing eight such pile models that were collectively integrated with a common grillage under axial load conditions revealed a 1.42-times-higher bearing capacity compared to a control model of a shallow foundation (sole size:  $60 \times 24$  cm; laying depth: 80 cm). This advantage was ascribed to the expansion of the pile trunk facilitated by the absorption of sand particles by concrete from the well walls, their adherence to the surface, and the resistance characteristics of the rough edges of the trunk against ground penetration. The authors projected a forecasted settlement of 5 mm under design loads for a building constructed on such pile foundations (as opposed to up to 15 mm for the comparative shallow foundation).

An evaluation of the load-bearing capacity of bored piles in sandy soil incorporating expansion additives [23] revealed that the utilization of an expanding concrete mixture resulted in a heightened lateral resistance (up to 15–50%) and a diminished settlement (up to 25%) across most load ranges compared to conventional concrete piles. In essence, abbreviated expanding piles facilitated by specialized expanding mixtures demonstrated a commensurate load-bearing capacity to longer conventional concrete piles. This outcome was attained by augmenting the surface area of the trunk in contact with the surrounding soil, leading to a reduction in the required length of the piles. Consequently, this reduction in pile length translated to cost savings and a reduction in construction time.

Experiments involving bored piles installed using systems featuring an expansion body [24] along with concrete filled with crushed stone resulted in an additional enlargement of the piles' diameter by 0.4–0.8 m through high-pressure air injection. Piles thus broadened exhibited a 33% greater resistance to surface friction under static axial loads and a 40% increase in resistance during withdrawal compared to a pile without such widening.

Recommendations for the design and construction of flat-profile piles emphasize the significance of incorporating a coefficient to consider the increased load-bearing capacity of piles driven with the addition of loose materials [25]. These recommendations indicate that the bearing capacity of 5, 7, and 9 m flat-profile piles was respectively 1.27, 1.30, and 1.32 times greater when driven with loose materials compared to those without such additions. The most substantial impact of incorporating loose materials was observed in the case of the 9 m piles. The authors proposed specific quantities of loose material per pile, corresponding to 200, 380, and 460 kg for piles with lengths of 5, 7, and 9 m, respectively.

In another approach described in [26], the method involves the construction of a pile–slab foundation with crushed-stone widening beneath the lower ends of the piles. Piles measuring 8 m in length and 53 cm in diameter were installed within excavation pits with widening created in their lower sections through the gradual compaction of crushed stone totaling 1 cubic meter beneath each pile. The widening beneath the piles' lower ends measured 100 cm.

This innovative method significantly enhanced the load-bearing capacity of piles by creating widening beneath their tips, optimally distributing the load between the foundation's slab and the piles. It resulted in a reduction of up to 50% in the required number of piles. The distances between piles in the foundation were established at 5 times the pile diameter ( $5d'$ ), where  $d'$  represents the pile diameter. The design of such a pile–slab foundation with crushed-stone widening for a 16-story building led to up to 20% in cost savings compared to the design involving driven prismatic piles, each measuring 17 m in length and having a cross-sectional dimension of  $30 \text{ cm} \times 30 \text{ cm}$ .

In [27], features related to the construction of cast-in-place piles with dual widening in their lower sections are discussed. These piles were formed by sequentially filling the excavation with large rigid materials (such as coarsely crushed stone) in layers that were compacted with a lengthy tamper featuring a pointed angle ranging from 120 to 180 degrees. This process resulted in the creation of a broadened section in the lower part of

the pile without significant lateral expansion. Subsequently, a finer rigid material (crushed stone or fine gravel) was added on top of this widening and compacted using a tamper with a pointed angle ranging from 25 to 90 degrees, resulting in an upper widening. The load-bearing capacity of the cast-in-place piles with dual widening in the lower section surpassed that of piles without widening by 1.5–3.0 times due to increased soil resistance along the pile's lateral surface.

Furthermore, [27] presents an alternative approach for constructing piles with dual widening that involved driving a pile into the well after the expansions were created. The researchers noted that such piles also exhibited a high load-bearing capacity.

The collective works [1–27] underscore the substantial role of both geometric widening within the pile shaft and the application of rigid material backfills in enhancing the load-bearing capacity of piles. However, there is a notable absence of research addressing the combined impact of these factors on load-bearing capacity within a specific pile structure type. Additionally, researchers have overlooked the influence of the rigid material type on pile resistance and the energy intensity of pile driving despite the wide variety of rigid materials used during pile installation.

Recognizing the significance of these issues, our research endeavors have included experimental investigations employing driven piles with one to four flat widenings along the shaft length. This research occurred in two stages. The first stage assessed the impact of the number of widenings on the load-bearing capacity and pile-driving energy intensity, while the second stage evaluated the influence of the type of rigid and soil material placed beneath the pile widenings on the load-bearing capacity and energy-related parameters. The results of the first stage are presented in [8], and the second stage is elucidated in this paper. These experiments were conducted under laboratory conditions and utilized pile models and four types of backfill materials: loam, sand, gravel, and crushed stone. The research aimed to investigate the influence of backfill materials composed of soil and rigid substances on the energy intensity of pile driving and the resistance to static loads while taking into account piles featuring multiple shaft widenings.

From a comprehensive perspective, these studies are oriented toward advancing the theory of pile foundation modeling with the intent to utilize their outcomes in addressing challenges related to delineating patterns of variation in energy and power parameters within pile arrangements featuring trunk widening with the inclusion of rigid material. The acquired research findings are poised to facilitate a preliminary evaluation of the viability of this technology for constructing widened piles, enabling the identification of qualitative characteristics applicable to field conditions. The experimental results will serve as a foundation for establishing conditions conducive to modeling the process of driving scale models with the addition of hard material, paralleling the process of driving full-scale piles of analogous shape with the inclusion of hard material.

## 2. Materials and Methods

Experimental studies were carried out in the geotechnical laboratory of the M.Kh. Dulaty Taraz Regional University.

The methodology employed for modeling experimental studies primarily relied upon the principles of similarity theory, aiming to furnish comparative data on the behavior of piles and discern qualitative patterns in their performance under various loads. To replicate the process of driving piles into soil under controlled laboratory conditions, the following similarity conditions were established:

- The relative residual failure of the pile model during driving must correspond to the relative residual failure when driving a full-scale pile  $\Delta S_{0m} = \Delta S_{0n}$ ;
- The ratio of the volume of the deformed soil zone formed around the pile model to the volume of the model should correspond to the ratio of the volume of the deformed soil zone formed around the full-scale pile to the volume of the pile  $V_{um}/V_m = V_{un}/V_n$ ;

- The specific energy intensity of the immersion of the pile model in one blow of the hammer (hammer model) must correspond to the specific energy intensity of the immersion of a full-scale pile in one blow of a pile hammer  $E_{vm} = E_{vn}$ ;
- The ratio of the mass of the hammer model (striker) to the mass of the pile model must correspond to the ratio of the mass of the hammer impact part to the mass of the pile  $Q_m/q_m = Q_n/q_n$ .

where  $\Delta S_{0m}$  and  $\Delta S_{0n}$ , respectively, are the relative residual failures of the model and the pile;  $V_{um}$  and  $V_{un}$ , respectively, are the volumes of deformed soil zones around the model and the pile;  $V_m$  and  $V_n$ , respectively, are the volumes of the model and the pile;  $E_{vm}$  and  $E_{vn}$ , respectively, are the specific impact energies spent on moving the model and the pile by the amounts  $S_{0m}$  and  $S_{0n}$ ;  $S_{0m}$  and  $S_{0n}$ , respectively, are the residual failures of the model and the pile;  $Q_m$  and  $Q_n$ , respectively, are the mass of the hammer (hammer model) and the impact part of the hammer; and  $q_m$  and  $q_n$ , respectively, are the mass of the model and the pile.

These stipulated conditions provide a rational basis for determining modeling parameters in the investigation of the pile submersion, energy intensity, and bearing capacity of laboratory models.

### 2.1. Models of Piles with Widening

Models of piles with shaft widenings were constructed using wooden beams. The model scale of the piles was set at 1:10. Typically, a pile model with multiple shaft widenings comprises a prismatic section and widening portions resembling inverted flat truncated pyramids. In the experiments, pile models with 2, 3, and 4 shaft widenings were employed (see Figure 1). The height of each model widening measured 100 mm, and the top dimensions of the widening were  $20 \times 45$  mm. The prismatic portion of the pile possessed a square cross-section with dimensions of  $20 \times 20$  mm. The overall shaft length of the pile model extended to 500 mm. Detailed geometric specifications and the mass of the pile models are presented in Table 1 for reference.

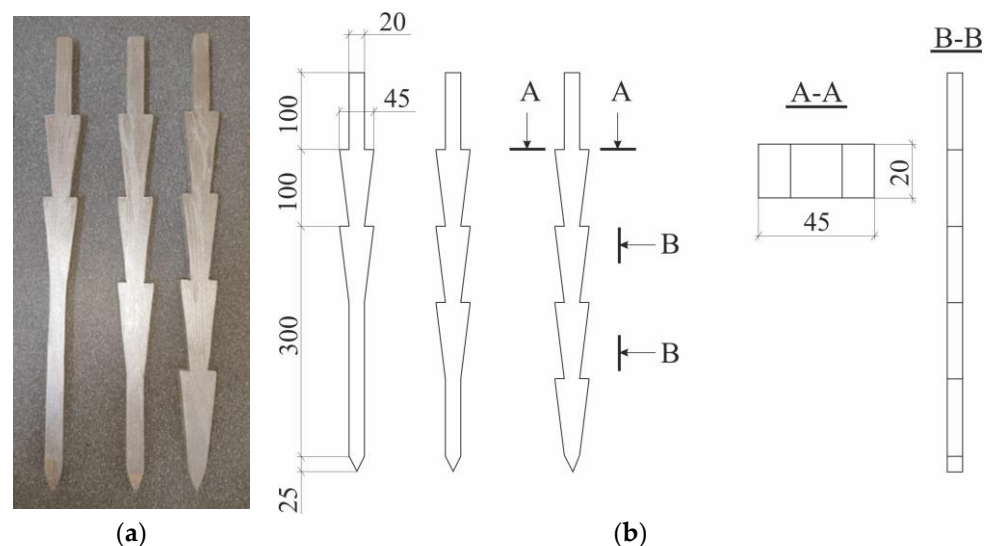


**Figure 1.** General view (a) and scheme (b) of models of piles with widenings.



**Table 1.** Geometric parameters of pile models and their weights.

Pile Model View	Geometric Parameters, mm					Weight, g
	Shaft Length	Tip Length	Shaft Cross-Section Dimensions	Widening Width	Widening Height	
Pile with 2 widenings	500	15	20 × 20	45	100	135
Pile with 3 widenings						147
Pile with 4 widenings						158

## 2.2. Preparation and Parameters of Soil Base and Rigid Material for Backfill

The basis soil employed in the test consisted of disturbed light sandy loam. The soil type classification adhered to the guidelines specified in the relevant standard [28]. To prepare the clayey soil, the following procedures were followed: Initially, the soil underwent sieving through a mesh with a 2 mm hole diameter. Subsequently, the prepared soil was adequately moistened to achieve a moisture content of 10% by weight. The moisture content of the soil was determined in compliance with the relevant standard [29]. The dampened soil was methodically arranged in a tray in successive layers, with each layer measuring 10 cm in thickness. Each layer of soil was meticulously leveled and compacted. In total, seven layers of soil were deposited. In each experimental iteration, the physical and mechanical properties of the soil were ascertained in accordance with the standard guidelines [29] utilizing the penetration method facilitated by the PSG MG-4 device. Detailed soil characteristics are provided in Table 2.

**Table 2.** Physical and mechanical characteristics of the soil base.

Description	Value
Water content, $\omega$ , %	9.94–11.86
Soil density, $\rho$ , g/cm <sup>3</sup>	1.29–1.47
Liquid limit, $W_L$ , %	25.05–25.17
Plastic limit, $W_p$ , %	13.23–15.03
Plasticity index, $I_p$	9.93–11.96
Maximum penetration resistance, $P_{max}$ , MPa	0.268–0.275
Compaction ratio, $K$	0.81–0.84
Wetness index, (degree) $I_w$	1.73–1.98
Strain modulus, $E_0$ , MPa	15.2–16.0
Angle of internal friction, $\phi$ , grade	13.1–13.2
Intercept cohesion, $c$ , MPa	0.0302–0.0310

Throughout the experiments, variations in the soil moisture content of the base over time were considered. This was monitored by measuring the initial soil moisture (before commencing the experiments) and the final soil moisture (after concluding the experiments) and employing a drying process until a constant mass was achieved in adherence to the specifications outlined in the standard [29].

This study utilized common soil and construction materials prevalent in the region as rigid backfill material (Figure 2):

- Light sandy loam with a disturbed structure; the type of soil was established in accordance with the requirements of the standard [28] (water content  $w = 1.14$ – $1.16\%$ );
- Medium-sized sand characterized by a homogeneous composition; the type and coefficient of heterogeneity of sand were determined in accordance with the requirements of the standard [28] (water content  $w = 1.12$ – $1.15\%$ );
- Gravel, which was selected in compliance with the criteria specified in the relevant standard [30] while taking into account the modeling scale (maximum particle size  $D = 5$  mm; ratio of gravel mass to sand mass: 35%/65%; water content  $w = 1.12$ – $1.15\%$ );
- Crushed stone adopted in accordance with the requirements of the standard [31] and considering the modeling scale (maximum particle size  $D = 5$  mm).

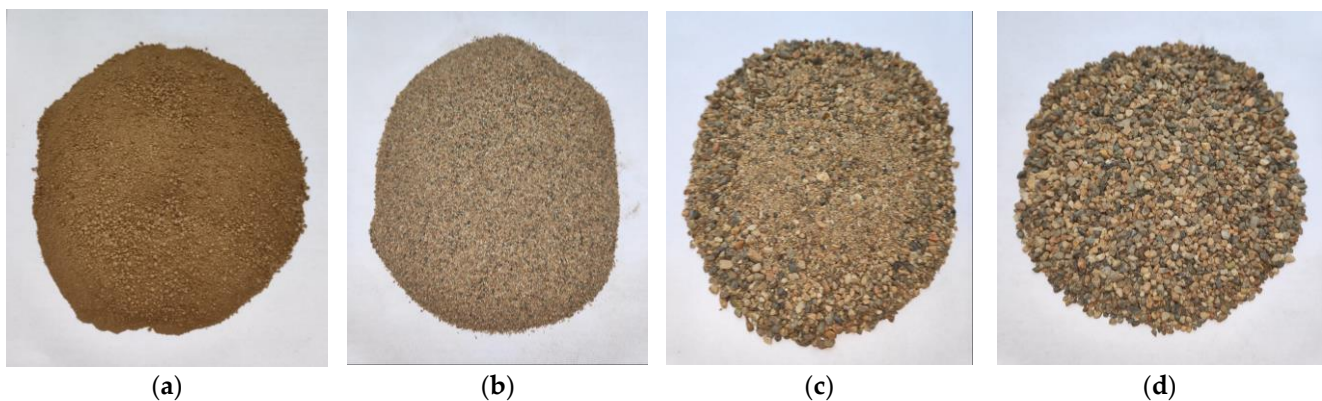


**Figure 2.** Types of soil and rigid materials used as backfill material. (a)—light sandy loam; (b)—medium-sized sand; (c)—gravel; (d)—crushed stone.

### 2.3. Parameters and Features of Equipment Operation

The experiments were carried out in a soil tray equipped with multi-purpose laboratory attachments (Figure 3). The tray had plan dimensions of  $150 \times 55$  cm and a height of 80 cm. Attachments allowed driving and static testing of the pile models in accordance with the requirements of the standard [32].

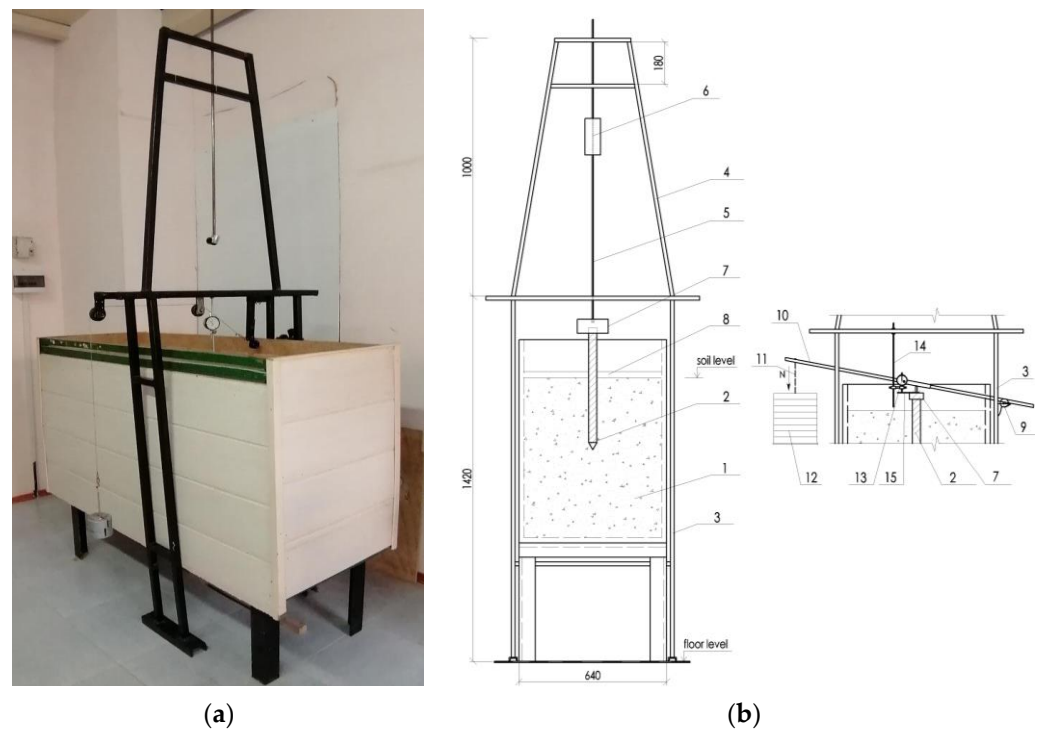


**Figure 3.** General view (a) and scheme (b) of the soil tray and attachments for driving and testing pile models. 1—Soil tray; 2—pile model; 3—inverted U-shaped lower frame; 4—upper frame with inclined racks; 5—guide rod; 6—hammer; 7—headrest; 8—removable guide beam; 9—hinged part of the lever system; 10—beam-lever; 11—cable; 12—container for cargo; 13—indicator; 14—rod for attaching the indicator; 15—cantilever plate.

The framework of the attachments was constructed using welded square metal profiles and, in the lower section, comprised two U-shaped frames with consoles resting on a concrete floor. In the upper portion, the equipment's frame included a singular frame with inclined racks, which were welded from below to horizontal metal elements connecting the lower frames to each other. Two beams at different levels in the upper frame had

through-holes allowing the passage of a guide rod designed for the descent of a hammer. The guide rod, composed of smooth reinforcement with a 10 mm diameter, was installed with its lower end into the headrest hole, which was mounted on the head of the pile model.

To ensure precise placement of the pile model's tip during hammering and to prevent rotation or deviation of the pile model during immersion, the tray was equipped with a removable guide beam. This guide beam consisted of two 40 mm wide wooden slats fastened together with wooden inserts between them, forming a slot in the central part for the pile model to pass through. The dimensions and shape of the slot corresponded to the shape and largest dimensions of the cross-section of the pile model.

To conduct tests involving static pressure loads on pile models, the tray attachments were equipped with a lever system. This lever system consisted of a hinged part, a lever beam, and a rope with a hook for holding the load. The hinged part comprised two ball bearing rollers mounted on a metal axial rod bolted to it and connected to a single hinge with a lever beam retainer. This retainer, due to the free rotation of the axial rod, could change the angle of inclination in the vertical direction and had screw clamps on the opposite side faces.

The lever beam, composed of a square metal profile with a length of 118 cm, was inserted into the lock of the hinged part and fixed with screw clamps. Another movable metal retainer with a hole in the lower part and a clamping screw in the upper part was inserted into the free end of the lever beam. This retainer, which was movable along the length of the lever beam, served to fix the tubular rod in a vertical position, transmitting force from the lever beam to the pile model. A metal ball with a 10 mm diameter was placed between the movable retainer and the tubular rod, ensuring strictly axial load transfer from the lever beam to the pile model.

The cable of the lever system was attached to the top of the lever beam. A container with a length of 620 mm and a diameter of 1.5 mm was suspended from a hook fixed in the lower part of the cable for placing pre-calibrated cargo. Placing the load in the container induced tension in the cable, transferring the pressing force to the pile model through the lever system of the tray.

To measure the settlement of the pile model when subjected to a load through the lever system, a digital hour-type indicator (HIC) with a division price of 0.001 mm was utilized. The indicator was fixed on a rod attached to the beam of one of the lower frames of the attachments with its lower end resting against the beam lever of the equipment's lever system.

To subject pile models to static axial loads, the tray attachment was configured with a lever system. This lever system encompassed a pivotal component, a beam lever, and a cable furnished with a hook designed for load application. The pivotal component afforded the beam lever the capacity to freely adjust its inclination angle in the vertical direction during both the application and removal of the load from the pile model. To ensure the precise transmission of axial loads from the beam lever to the pile model, a metal ball with a 10 mm diameter was interposed between the head of the pile model and the beam lever. The transmission of compressive force to the pile model via the tray's lever system was executed in a stepwise manner by employing calibrated weights.

#### 2.4. Test Procedure

The model piles were embedded in the soil through hammer driving to a nearly uniform depth, with each blow delivering a consistent amount of energy (refer to Figure 4a). To accomplish this, the hammer for driving the pile models had a weight of 600 g, and the drop height was 50 cm. This ensured consistent driving energy for the model piles with each impact. The pile models were driven until they reached a total depth of 425–426 mm. During the driving process, the count of hammer blows was recorded, and the residual settlement at the end of driving was measured. Subsequently, after the lower widening of the pile model had been fully submerged in the soil, backfill material was introduced



onto the buried widening around the pile shaft (as depicted in Figure 5). To facilitate the filling process and to prevent the bulk material from dispersing laterally during driving, a funnel-like device was employed. While being driven in, the bulk material occupied the open space around the pile shaft created by the lower widening. The upper widening further facilitated the insertion of the bulk material into voids, ultimately pushing and embedding the backfill material deeper into the soil. Upon the completion of the driving process, any excess added material remaining at the soil surface was removed. The volume of bulk material effectively buried within the soil was quantified.

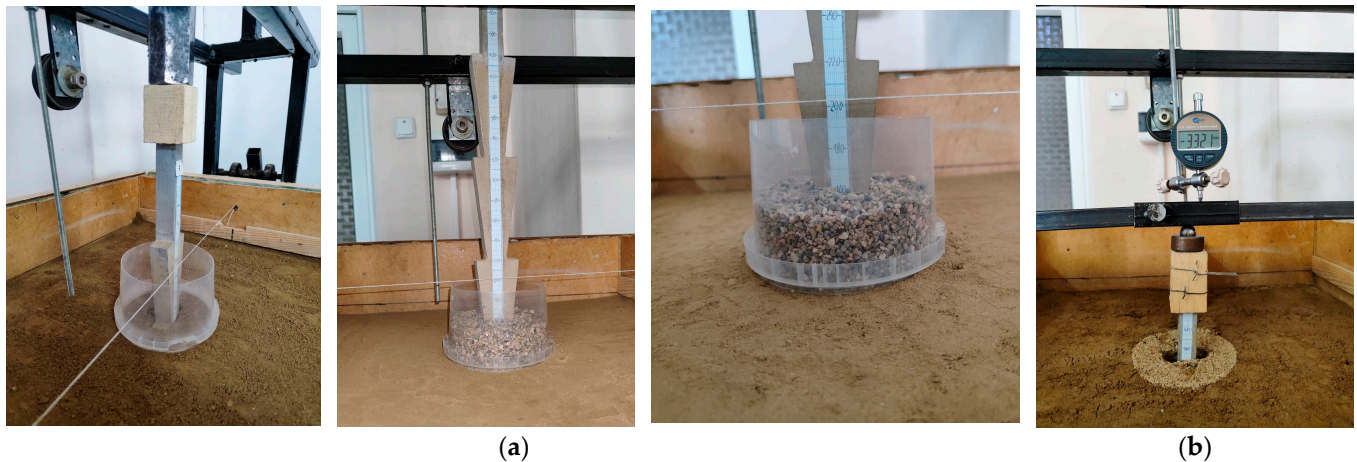


**Figure 4.** Fragments of driving (a) and static tests (b) of pile models with widenings and backfilling with rigid material.

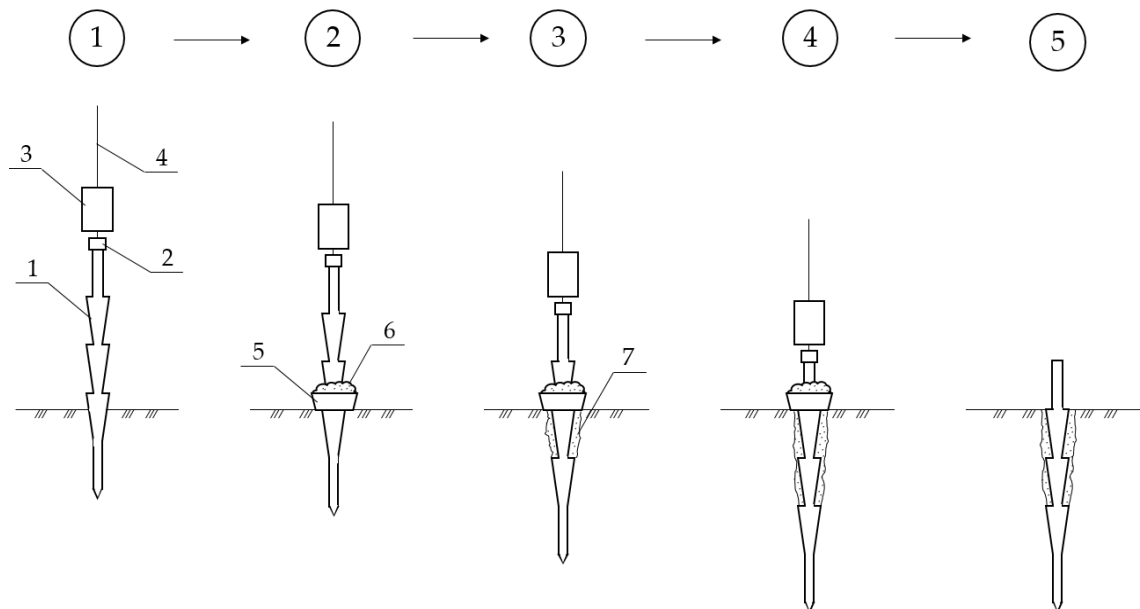


**Figure 5.** Schematic view of driving piles with shaft widenings with a backfill of soil or rigid material. 1—Pile with widening; 2—headrest; 3—hammer; 4—guide rod; 5—funnel; 6—backfilling composed of soil or rigid material; 7—compacted rigid material.

An axial load test on the pile models was executed in strict compliance with the stipulations outlined in the relevant standard [32] as well as in adherence to the fundamental principles established in the comprehensive guidelines [33]. Loads were incrementally applied to the pile models in a staged manner following the attainment of the requisite level of conditional stabilization for deformations at each loading stage. Vertical deformations (specifically, settlements) of the pile models were adjusted to a minimum of 40 mm. These

settlement deformations were meticulously quantified using a precisely calibrated digital dial indicator designated as IChTs-12 and boasting a remarkable accuracy level of 0.001 mm (as illustrated in Figure 4b).

The bearing capacity of the pile models under an axial load was determined based on the following test results:

(1) In alignment with the criteria specified in the comprehensive guidelines [34] and employing the formula:

$$F_d = \gamma_c \frac{F_{u,n}}{\gamma_g}, \quad (1)$$

where  $\gamma_c$  is the coefficient of operating conditions of the pile (taken as equal to 1.0 under an axial load),  $F_{u,n}$  is a standard value for the ultimate resistance of the pile (taken as equal to its lowest ultimate resistance according to test results, N), and  $\gamma_g$  is the soil reliability coefficient (taken as equal to 1.0).

(2) In accordance with the requirements of the set of rules [33] according to the formula:

$$R_{c;k} = \frac{(R_{c;m})_{\min}}{\xi_2}, \quad (2)$$

where  $R_{c;k}$  is the characteristic resistance of soil to compression in the limiting state of bearing capacity,  $(R_{c;m})_{\min}$  is the smallest value of the measured value of soil compression resistance depending on the number of tests of the pile models,  $\xi_2$  is the correction coefficient for assessing the test results for the pile models with a static load (taken as equal to 1.05 (at  $n = 3$ )), and  $n$  is the number of tests of the pile models.

### 3. Research Results and Discussion

#### 3.1. Test Results of Pile Models with 4 Widening

The test results of driving pile models with four widenings are presented in Figure 6 and Table 3. For a comparative assessment of the test results, the following indicators were adopted:

- The overall energy applied by the hammer ( $E$ ) spent on burying the pile model to the required depth;
- The energy intensity of the hammer for driving a pile model ( $E_v$ ) expressed per unit volume of the portion of the pile buried within the soil (calculated as the ratio of the total energy expended for driving a pile model to the volume of the section buried in the soil);
- The volume of backfilling material ( $v_p$ ) introduced into the vicinity of the pile during the driving process;
- An indicator of the enhanced energy intensity during driving ( $P_e$ ) calculated as the ratio of the total driving energy required for the pile model with the inclusion of rigid material to the total driving energy necessary for the pile model without any backfill material.

The experimental findings presented above revealed several key observations regarding the driving of pile models featuring four widenings:

- Depending on the type of rigid material used as backfill, at the same depth of immersion, the experimental pile models (with backfill) exhibited a 1.36–1.54-times-higher energy intensity during driving compared to the control pile model (without backfill).
- The energy intensity of pile driving per unit volume was 1.356–1.535 times greater for pile models with backfill compared to those without any backfill material.
- When driving pile models to the same depth, the volume of backfill material varied, with loam requiring the least ( $62 \text{ cm}^3$ ), sand the most ( $136 \text{ cm}^3$ ), and crushed stone ( $96 \text{ cm}^3$ ) and gravel ( $132 \text{ cm}^3$ ) falling in between.

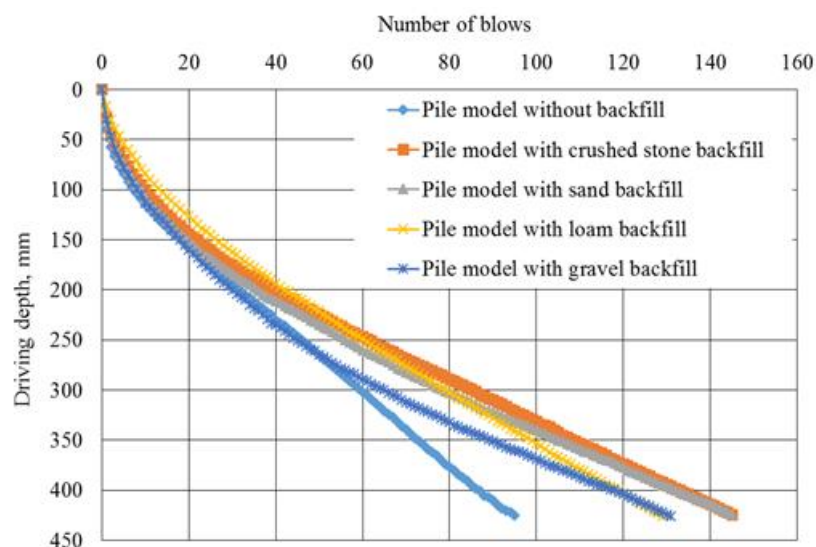


Figure 6. Pile models driven with 4 widenings.

Table 3. Driving test results of pile models with 4 widenings.

Pile Model	Backfilling Material Volume, $v_p$ , $\text{cm}^3$	Total Energy of Pile Driving, $E$ , J (Number of Blows)	Immersion Depth of Pile, $L$ , mm	Piles' Immersed-Part Volume, $V$ , $\text{cm}^3$	Energy Intensity of Pile Driving per Unit Volume, $E_{v_r}$ , $\text{J}/\text{cm}^3$	Indicator of Increasing Energy Intensity of Driving, $P_e$
Pile model with four widenings (without backfill)	-	279.59 (95)	425	215.0	1.300	-
Pile model with loam backfill	62	379.65 (129)	426	215.4	1.763	1.36
Pile model with crushed stone backfill	96	429.68 (146)	426	215.4	1.995	1.54
Pile model with gravel backfill	132	385.53 (131)	426	215.4	1.790	1.38
Pile model with sand backfill	136	429.68 (146)	426	215.4	1.995	1.54

As can be seen from the test results (Table 3), the spending on crushed stone for backfill in driving a model pile was 1.38 times less than the spending on gravel. However, at the same time, the total energy intensity for driving a model pile with crushed stone was 11.45% more than when driving a model pile with gravel. This can be attributed to the fact that crushed stone, unlike gravel, has a more consistent size distribution with fewer smaller particles. Moreover, the surface of crushed stone particles exhibits substantial roughness and irregularities, impeding their relative movement when impacting a pile model and consequently increasing soil resistance. Hence, between these two types of coarse materials, the preference for driving pile models should be given to gravel mixtures over crushed stone. This choice is further justified by the lower cost of gravel compared to crushed stone.

A comparison of the test results pertaining to the driving of a pile model using fine-grained backfill materials (loam and sand) revealed that the consumption of loam was 2.19 times less than that of sand (as indicated in Table 3). With the reduced usage of loam, driving a model pile incurred a lower total energy expenditure from the hammer (1.13 times less) in comparison to driving a model pile filled with sand. This distinction, in our assessment, was attributed to the cohesive nature of loam particles, which exhibited better interconnection. Consequently, loam was less mobile within the soil when subjected to the impact of the pile model, leading to a smaller volume of loam being incorporated into the soil and a subsequent reduction in the energy intensity required to drive the pile model.

The resistance of the pile models with four widenings was assessed based on the results of their static tests with axial loads (Table 4). The dependence of the settlement of pile models under an axial load is shown in Figure 7.

**Table 4.** Values for the  $F_d$ ,  $R_{c;k}$ ,  $F_d^v$ , and  $P_d$  indicators of pile models with 4 widenings.

Pile Model	Load-Bearing Capacity, $F_d$ , N	Characteristic Resistance of Soil to Compression at the Limiting State of Bearing Capacity, $R_{c;k}$ , N	Load-Bearing Capacity per Unit Volume, $F_d^v$ , V/cm <sup>3</sup>	Resistance-Increasing Index, $P_d$
Pile model with four widenings (without backfill)	272.8	259.81	1.269	-
Pile model with loam backfill	388.0	369.52	1.801	1.42
Pile model with crushed stone backfill	371.9	354.19	1.727	1.36
Pile model with gravel backfill	425.8	405.52	1.977	1.56
Pile model with sand backfill	457.6	435.81	2.124	1.68

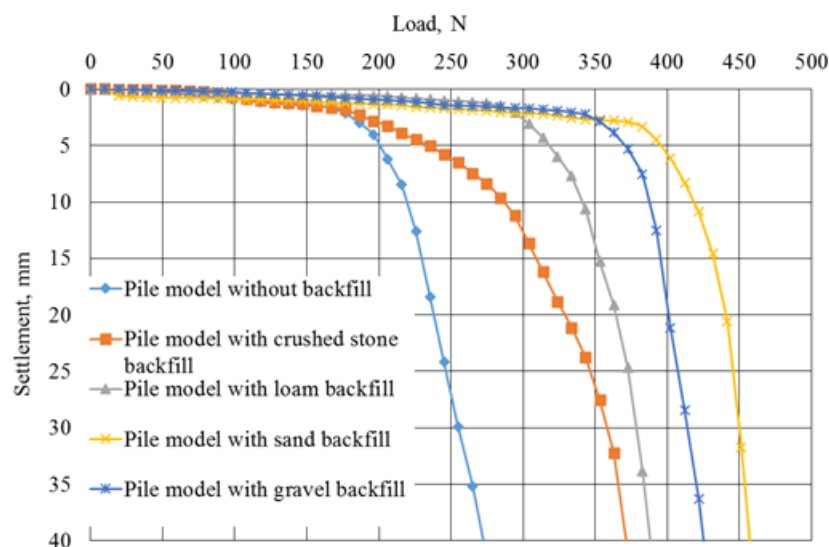


**Figure 7.** Settlement versus static load for pile models with 4 widenings.

The following indicators were adopted for the comparative assessment of the test results (Table 4):

- Load-bearing capacity  $F_d$ , established in accordance with the provisions of the regulatory document [32];
- Load-bearing capacity per unit volume  $F_d^v$ , i.e., the ratio of the load-bearing capacity of the pile model to the buried volume of the pile in the soil;
- Resistance-increasing index  $P_d$ , which was the ratio of the resistance of the pile model with the addition of rigid material to the bearing capacity of the pile model without any addition.

The test results indicated that pile models with backfilling, depending on the type of backfill material, exhibited a greater load-bearing capacity (1.36–1.68 times) compared to the control pile models (without backfilling) while maintaining the same settlement values. The highest load-bearing capacity values were observed in pile models driven with added sand and gravel, whereas the lowest values were found in piles with added crushed stone and loam (refer to Table 4). We attributed the increased resistance of pile models with sand and gravel backfill to the substantial volumes of backfill material introduced into the soil during driving. Specifically, the volume of gravel filled into the soil was 1.38 and 2.13 times

greater than the volume of crushed stone and loam, respectively. Similarly, the volume of sand was 1.42 and 2.19 times greater, respectively. The introduction of a larger volume of backfill material during driving contributed to enhanced soil compaction around the widening of the models, thereby increasing their bearing capacity.

Comparatively, the load-bearing capacity of a pile model with sand filling was 1.23 and 1.18 times greater than pile models with crushed stone and loam addition, respectively. Similarly, the load-bearing capacity of a pile model with gravel addition was 1.14 and 1.10 times greater, respectively.

Considering the advantages demonstrated by pile models driven with sand and gravel, subsequent tests involving pile models with two and three shaft widenings were exclusively conducted using these materials, as they proved more effective in ensuring the load-bearing capacity of the piles.

### 3.2. Test Results of Pile Models with Three Widenings

The test results for the driving and static testing of pile models with three widenings are presented in Figures 8 and 9 and Tables 5 and 6.

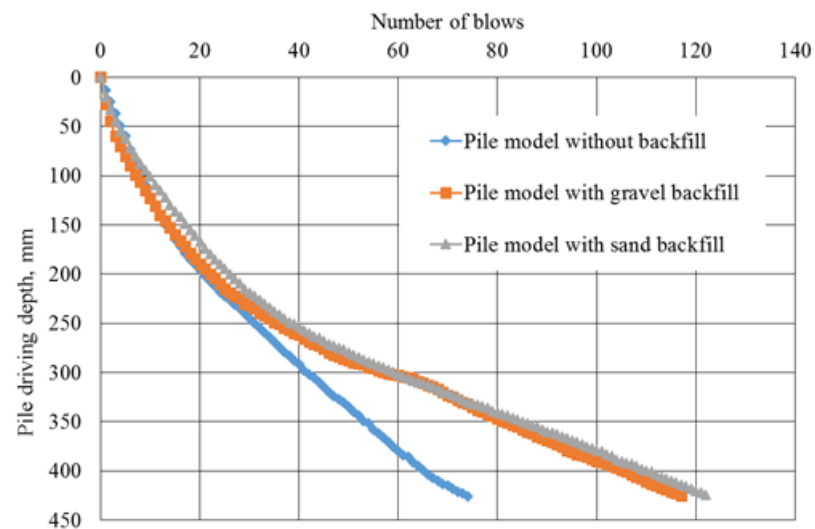


Figure 8. Pile models driven with 3 widenings.

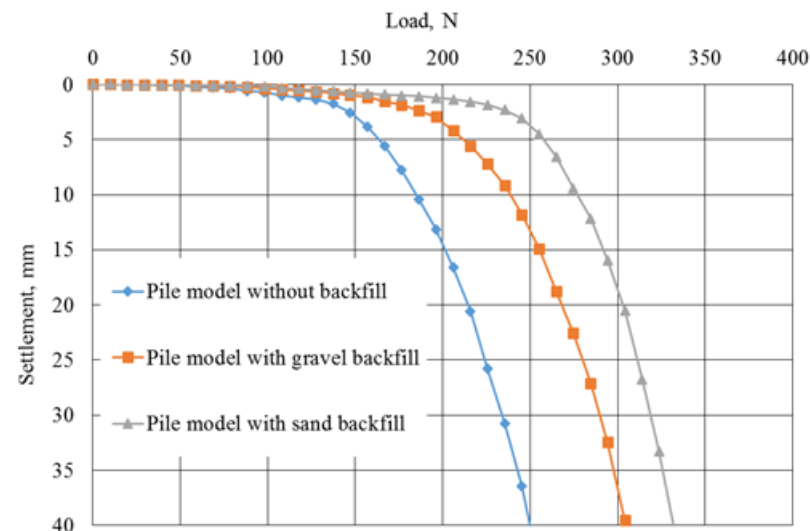


Figure 9. Static test results for pile models with 3 widenings.



**Table 5.** Driving test results for pile models with 3 widenings.

Pile Model	Backfilling Material Volume, $v_p$ , $\text{cm}^3$	Total Energy of Pile Driving, $E$ , J (Number of Blows)	Immersion Depth of Pile, $L$ , mm	Piles' Immersed-Part Volume, $V$ , $\text{cm}^3$	Energy Intensity of Pile Driving per Unit Volume, $E_v$ , $\text{J}/\text{cm}^3$	Indicator of Increasing Energy Intensity of Driving, $P_e$
Pile model with three widenings (without backfill)	-	217.78 (74)	426	215.4	1.011	-
Pile model with gravel backfill	85	344.33 (117)	425	215.0	1.602	1.58
Pile model with sand backfill	88	361.99 (123)	426	215.4	1.681	1.66

**Table 6.** Values for the  $F_d$ ,  $R_{c;k}$ ,  $F_d^v$ , and  $P_d$  indicators of pile models with 3 widenings.

Pile Model	Load-Bearing Capacity, $F_d$ , N	Characteristic Resistance of Soil to Compression at the Limiting State of Bearing Capacity, $R_{c;k}$ , N	Load-Bearing Capacity per Unit Volume, $F_d^v$ , $\text{N}/\text{cm}^3$	Resistance-Increasing Index, $P_d$
Pile model with three widenings (without backfill)	255.06	242.91	1.184	-
Pile model with gravel backfill	313.92	298.97	1.460	1.23
Pile model with sand backfill	333.54	317.66	1.548	1.31

The energy intensity of the hammer for driving pile models with added sand and gravel significantly exceeded the intensity for driving them without adding any bulk material (Table 5). Driving a pile model with sand addition rather than with gravel backfilling was more energy-consuming (by 5.13%). This difference was due to the unequal volume of sand and gravel added to the soil during the model driving. Consequently, 3.53% more energy was expended on driving a pile model with sand relative to gravel backfilling, leading to an escalation in the energy intensity during pile driving when sand was used.

The bearing capacity of pile models with gravel and sand backfilling was higher than the bearing capacity of a pile model without backfilling (Table 6). At the same time, the greatest load-bearing capacity belonged to the model of the pile driven with sand, which was 6.25% greater than that of the model with gravel.

### 3.3. Test Results for Pile Models with Two Widenings

The results of driving and static testing of pile models with two widenings are shown in Figures 10 and 11 and Tables 7 and 8.

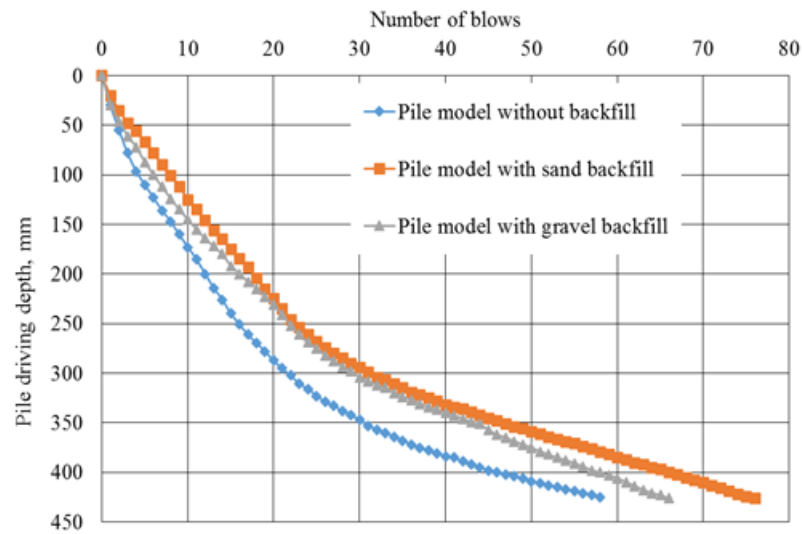


Figure 10. Pile models driven with 2 widenings.

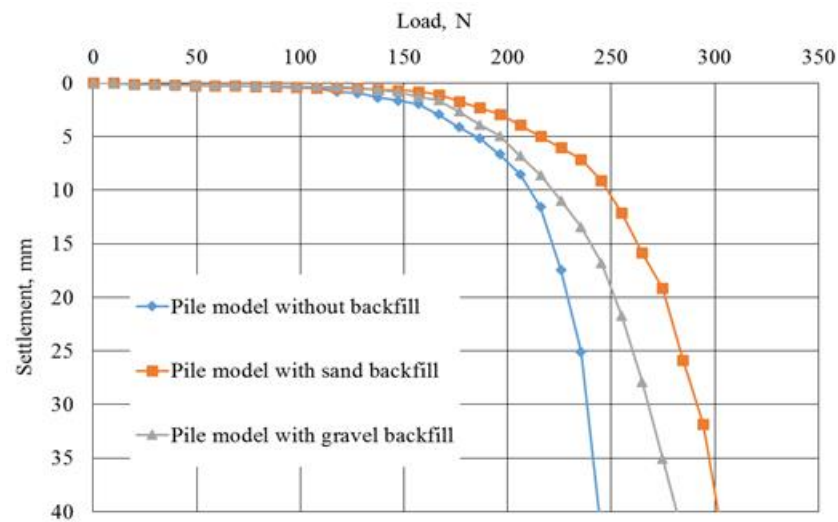


Figure 11. Static test results for pile models with 2 widenings.

Table 7. Driving test results for pile models with 2 widenings.

Pile Model	Backfilling Material Volume, $v_p$ , $\text{cm}^3$	Total Energy of Pile Driving, $E$ , J (Number of Blows)	Immersion Depth of Pile, $L$ , mm	Piles' Immersed-Part Volume, $V$ , $\text{cm}^3$	Energy Intensity of Pile Driving per Unit Volume, $E_v$ , $\text{J}/\text{cm}^3$	Indicator of Increasing Energy Intensity of Driving, $P_e$
Pile model with two widenings (without backfill)	-	170.69 (58)	425	215.0	0.794	-
Pile model with gravel backfill	40	194.24 (66)	426	215.4	0.902	1.14
Pile model with sand backfill	42	223.67 (76)	426	215.4	1.038	1.31

**Table 8.** Values for the  $F_d$ ,  $R_{c;k}$ ,  $F_d^v$ , and  $P_d$  indicators of pile models with 2 widenings.

Pile Model	Load-Bearing Capacity, $F_d$ , N	Characteristic Resistance of Soil to Compression at the Limiting State of Bearing Capacity, $R_{c;k}$ , N	Load-Bearing Capacity per Unit Volume, $F_d^v$ , V/cm <sup>3</sup>	Resistance-Increasing Index, $P_d$
Pile model with two widenings (without backfill)	244.4	232.76	1.137	-
Pile model with gravel backfill	281.8	268.38	1.308	1.15
Pile model with sand backfill	301.7	287.33	1.401	1.23

The energy intensity of driving pile models with added sand and gravel exceeded the intensity of pile driving without adding bulk material (Table 7). Moreover, 15.2% more energy was spent on driving a pile model with sand addition than with gravel addition. This increased energy expenditure on driving a pile model with sand can be attributed to the fact that the consumption of sand during the pile driving process exceeded that of gravel by 5%, leading to the elevated energy intensity during pile driving when sand was employed.

It was evident from the test results that the load-bearing capacity of the pile models filled with gravel and sand exceeded that of pile models lacking any backfill material (as outlined in Table 8). Notably, the pile model driven with sand exhibited the highest load-bearing capacity, surpassing the pile model with gravel backfilling by 7.06%.

### 3.4. Test Results Comparison of Pile Models with 2–4 Widenings

A comparison of the test results of driving pile models with 2–4 widenings buried with sand and gravel showed the influence between the number of widening in pile models and the amount of backfilling material. An increase in the number of widening led to an increase in the bulk material entrained by their widening into the soil (Table 9).

**Table 9.** The spending of backfilling ( $v_p$ ) during the driving of pile models with 2–4 widenings.

Backfilling Type	Spending of Backfilling $v_p$ , cm <sup>3</sup> , during the Driving of Pile Models with the Number of Widenings		
	2	3	4
Gravel	40	85	132
Sand	42	88	136

According to Table 9, the correlation dependencies  $\frac{v_p}{v_u} = f(n)$  were established (where  $v_u$  is the volume of widening of the pile model (backfilled volume), m<sup>3</sup>; and  $n$  is the number of widenings in the pile model), which are described by the linear function (3) (Figure 12):

$$v_p = tn + w, \quad (3)$$

where  $t$  and  $w$  are the coefficients accepted according to Table 10 and  $n$  is the number of widenings in the pile model.

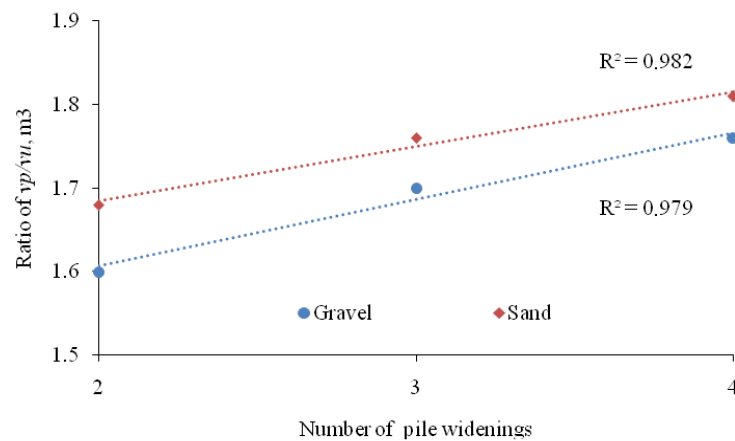


**Figure 12.** Dependence of the ratio  $\frac{v_p}{v_u}$  on the number of widenings in the pile model.

**Table 10.** Coefficients  $t$  and  $w$  in Equation (3).

Backfilling Type	Coefficient Values		Approximation Index $R^2$
	$t$	$w$	
Gravel	0.08	1.4467	0.979
Sand	0.065	1.555	0.982

Increasing the number of widenings in the pile models caused an increase in the energy intensity of their driving ( $E_v$ ) (Table 11 and Figure 13). This regularity is described by the dependency given in Equation (4).

$$E_v = pn + s, \quad (4)$$

where  $p$  and  $s$  are the coefficients accepted according to Table 12 and  $n$  is the number of widenings in the pile model.

**Table 11.** Energy intensity of pile driving ( $E_v$ ) per unit volume of pile models with 2–4 widenings.

Backfilling Type	Values of Energy Intensity $E_v$ Related to Pile Models with the Number of Widenings		
	2	3	4
Gravel	0.902	1.602	1.790
Sand	1.038	1.681	1.995

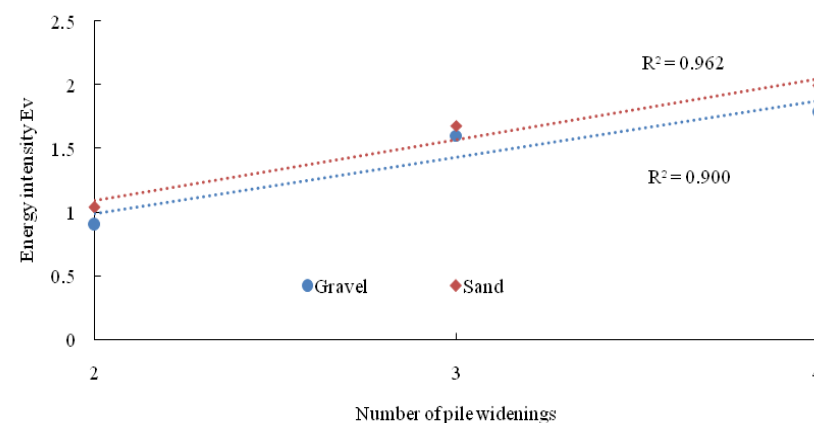


**Figure 13.** Energy intensity of pile driving ( $E_v$ ) versus the number of widenings in the pile model.

**Table 12.** Coefficients  $p$  and  $s$  in Equation (4).

Backfilling Type	Coefficient Values		Approximation Index $R^2$
	$p$	$s$	
Gravel	0.444	0.099	0.900
Sand	0.478	0.135	0.962

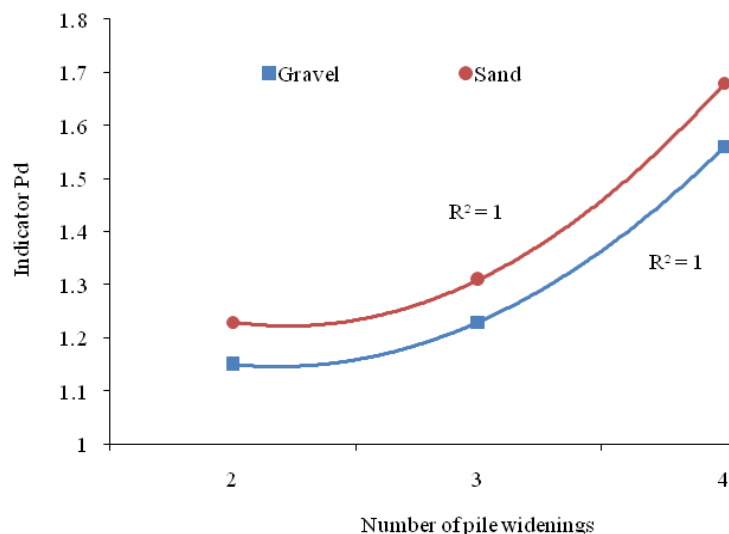
The load-bearing capacity of the pile models increased with their number of widenings (Table 13). This regularity is well described by a polynomial function of the second degree (5) (Figure 14).

$$p_d = qn^2 - dn + m, \quad (5)$$

where  $q$ ,  $d$  and  $m$  are the coefficients accepted according to Table 14 and  $n$  is the number of widenings in the pile model.

**Table 13.** Values of the resistance-increasing index  $P_d$  for pile models with 2–4 widenings.

Backfilling Type	$P_d$ Index Values Related to Pile Models with the Number of Widenings		
	2	3	4
Gravel	1.15	1.23	1.56
Sand	1.23	1.31	1.68

**Figure 14.** Resistance-increasing index ( $P_d$ ) versus pile models for the number of widenings.**Table 14.** Coefficients  $q$ ,  $d$  and  $m$  in Equation (5).

Backfilling Type	Coefficient Values			Approximation Index $R^2$
	$q$	$d$	$m$	
Gravel	0.125	0.295	1.32	1.0
Sand	0.145	0.355	1.44	1.0

### 3.5. Interrelation of the Present Test Results with the Experiments of the First Stage of Research

The comparative analysis of the energy intensity of driving pile models at the first stage of research [8] and similar parameters presented in this paper allowed us to formulate the following dependence:

$$E_{up} = K_e P_e E_p = K_{kp}^e E_p \quad (6)$$

where  $E_{up}$  is the energy intensity for driving a pile model with widening and a backfilling of bulk material (gravel or sand),  $K_e$  is an indicator of the comparative energy intensity of



a pile model with widenings and buried without backfilling bulk material [8],  $E_p$  is the energy intensity for driving a pile model without shaft widening (prismatic or pyramidal pile models), and  $K_{kp}^e$  is a coefficient that takes into account the number of widening in the pile model and the type of backfill of bulk material used in driving (Table 15).

**Table 15.**  $K_{kp}^e$  coefficient values.

Traditional Pile Type	$K_{kp}^e$ Coefficient Values Depending on the Backfilling Type and the Number of Widenings in the Pile			
	Backfilling Type	Number of Widenings		
		2	3	4
Prismatic pile with section dimensions of 20 × 20 cm	Gravel	2.440	4.361	4.595
	Sand	2.803	4.582	5.128
Prismatic pile with section dimensions of 30 × 30 cm	Gravel	0.855	1.533	1.615
	Sand	0.983	1.610	1.802
Pyramidal with cross-sectional dimensions of 30 × 30 cm at the top and 20 × 20 cm at the bottom	Gravel	1.391	2.481	2.608
	Sand	1.598	2.606	2.911

Equation (6) allows for a comparative assessment of the energy intensity of driving piles with shaft widenings relative to piles without widenings (prismatic and pyramidal piles). Table 15 shows that the energy intensity for driving piles with widenings and a backfilling of bulk material could be 1.4–5.1 times higher than the energy intensity for driving traditional piles without adding any bulk materials.

Formula (7), which was obtained similarly to Equation (6), allows for a comparative assessment of the load-bearing capacity of piles with shaft widenings relative to piles without widenings (prismatic and pyramidal piles).

$$F_{dup} = K_H p_d F_{dp} = K_{kp}^d F_{dp}, \quad (7)$$

where  $F_{dup}$  is the load-bearing capacity of a pile model with widenings and a backfilling of bulk material (gravel or sand),  $K_H$  is an indicator of the comparative load-bearing capacity of a pile with widenings and buried without adding any bulk material [8],  $F_{dp}$  is the load-bearing capacity of a pile model without shaft widenings (prismatic or pyramidal pile models), and  $K_{kp}^d$  is a coefficient that takes into account the number of widenings in the pile model and the type of backfilling of bulk material used in driving (Table 16).

**Table 16.**  $K_{kp}^d$  coefficient values.

Traditional Pile Type	$K_{kp}^d$ Coefficient Values Depending on the Backfilling Type and the Number of Widenings in the Pile			
	Backfilling Type	Number of Widenings		
		2	3	4
Prismatic pile with section dimensions of 20 × 20 cm	gravel	2.312	2.792	4.259
	sand	2.472	2.974	4.586
Prismatic pile with section dimensions of 30 × 30 cm	gravel	1.599	1.931	2.933
	sand	1.710	2.057	3.158
Pyramidal with cross-sectional dimensions of 30 × 30 cm at the top and 20 × 20 cm at the bottom	gravel	1.507	1.820	2.777
	sand	1.611	1.939	2.990

As can be seen in Table 16, the bearing capacity of piles with widenings that were driven with the addition of bulk material could be 1.5–4.6 times higher than the bearing capacity of traditional piles driven without adding any bulk materials.

### 3.6. Practical Application of the Obtained Results

The research results obtained through the conducted experiments hold significant relevance in engineering practice, particularly in the design and construction of pile foundations for buildings and structures. The findings from experiments evaluating the submersibility and energy intensity of pile-driving models provide valuable insights for making informed decisions regarding the selection of a pile-driving unit and its impact energy. This consideration is essential for the effective driving of piles with widenings to account for the type and volume of the applied fillings.

Moreover, the results of tests assessing the resistance of the studied piles under static axial loads offer valuable input at the design stage of pile foundations. Utilizing this data, a methodology for testing foundations composed of piles with widenings and the addition of soil and building materials can be formulated.

The proposed formulas enable a comparative evaluation of the energy intensity involved in driving piles with shaft widenings relative to piles without widenings, particularly prismatic and pyramidal piles. These formulas find utility in the variant design stage of foundations, facilitating the assessment of energy costs associated with the pile-driving process and the power parameters of piles with shaft widenings immersed in the ground with gravel and sand.

Consequently, the experimental data derived from the research results will contribute to the development of recommendations for executing pile work in construction. The adoption of this technology for installing piles with widenings in the construction of foundations, owing to their enhanced bearing capacity, has the potential to reduce the cost of foundation work (with forecast estimates suggesting up to 25–28% reduction). This in turn can lead to a reduction in the overall construction cost of the facility by approximately 17–19%, depending on its purpose. The introduction of the proposed technology for pile construction with extensions into construction practice thus presents an attractive advantage.

## 4. Conclusions

The results of experimental investigations detailed in this paper led to the following main conclusions:

(1) Piles with widenings driven with the addition of soil and rigid materials differed from higher (1.14–1.66 times) energy intensity than their driving without the mentioned addition. The energy intensity of pile driving was notably influenced by the choice of backfill material, with the lowest energy intensity observed when driving piles with loam backfill and the highest energy intensity evident when sand and crushed stone were used as backfill materials. Furthermore, the energy intensity of pile driving increased with the number of widenings in the pile, as the inclusion of a greater quantity of backfill material into the soil during the driving process was necessitated.

(2) The bearing capacity of piles with widenings driven with the addition of soil and rigid materials was higher (1.15–1.68 times) than the bearing capacity of piles driven without the use of filling material. This effect was more pronounced with an increasing number of widenings in the piles, as a larger volume of backfill material became integrated into the soil during the driving process.

(3) The type of backfill material affected the resistance of the piles to axial static loads. The greatest resistance was typical for piles driven with added sand, and the lowest with added crushed stone. Specifically, the load-bearing capacity of piles filled with sand surpassed that of piles filled with crushed stone and loam by factors of 1.23 and 1.18, respectively. Similarly, the bearing capacities of piles filled with gravel were 1.15 and 1.10 times higher, respectively. Based on the load-bearing capacity of the piles, it was preferable to use sand and gravel as backfill material.

(4) The energy intensity for driving piles with widenings and adding bulk materials was greater (1.4–5.1 times) than the energy intensity for driving traditional piles (prismatic and pyramidal piles) without adding bulk materials. In addition, the load-bearing capacity

of piles featuring widenings and driven with the inclusion of bulk materials surpassed that of traditional piles (lacking shaft widening) driven without any bulk material, exhibiting an increase ranging from 1.5 to 4.6 times.

(5) The correlation dependencies established based on the results of this research exhibited sufficient reliability and can be utilized for relatively approximate predictions of the energy and strength parameters of piles featuring shaft widenings buried in soil with gravel and sand backfill.

(6) The studies identified sand and gravel as the two most effective filling materials for enhancing the bearing capacity of piles with shaft widenings. Subsequent research will involve additional comparative studies incorporating numerical modeling to further investigate and validate these findings.

**Author Contributions:** Conceptualization, B.I. and A.Y.; methodology, B.I. and A.Y.; formal analysis, B.I., A.Y. and S.N.; writing—review and editing, B.I. and A.Y.; supervision B.I.; writing—original draft, A.Y. and S.N.; visualization, A.Y. and S.N.; funding acquisition, investigation, validation, A.Y.; resources, S.N. All authors have read and agreed to the published version of the manuscript.

**Funding:** This research was funded by the Science Committee of the Ministry of Science and Higher Education of the Republic of Kazakhstan (Grant No. AP15473198). Any opinions, findings, conclusions, or recommendations expressed in this material are those of the researchers and do not necessarily reflect the views of the Ministry of Science and Higher Education of the Republic of Kazakhstan.

**Data Availability Statement:** Data will be made available upon request. The data are not publicly available due to privacy.

**Acknowledgments:** The authors are grateful to the Science Committee of the Ministry of Science and Higher Education of the Republic of Kazakhstan.

**Conflicts of Interest:** The authors declare no conflict of interest.

## References

1. Zhang, S.; Liu, X.; Zhang, H.; Piao, C.; Niu, Y. Study on the Force Model of Squeezed Branch Piles Based on Surface Potential Characteristics. *Buildings* **2023**, *13*, 2231. [[CrossRef](#)]
2. Fedorov, V.S.; Kupchikova, N.V. Technologies for the installation of end widening of cast-in-place and finished piles and their influence on the shaping of foundation structures. *Eng. Constr. Bull. Casp. Reg. Sci. Tech. J.* **2019**, *1*, 40–56.
3. Murthy, V.N. *Geotechnical Engineering: Principles and Practices of Soil Mechanics and Foundation Engineering*; Marcel Dekker, Inc.: New York, NY, USA, 2002; pp. 741–751.
4. Bekbasaov, I.; Shanshabayev, N. Impact Dipping Pyramidal-Prismatic Piles and their Resistance to Pressure and Horizontal Load. *Period. Polytech. Civ. Eng.* **2021**, *65*, 909–917. [[CrossRef](#)]
5. Isabai, B.; Nurzhan, S.; Yerlan, A. Strength Properties of Various Types of Fiber-Reinforced Concrete for Production of Driven Piles. *Buildings* **2023**, *13*, 1733. [[CrossRef](#)]
6. Zhang, M.; Xu, P.; Cui, W.; Gao, Y. Bearing behavior and failure mechanism of squeezed branch piles. *J. Rock Mech. Geotech. Eng.* **2018**, *10*, 935–946. [[CrossRef](#)]
7. Zhu, W.-T.; Li, H.-Q.; Zeng, J.-Y.; Guan, W.-D. Applicability analysis of squeezed branch pile with different embedded depth of Boulder. *IOP Conf. Ser. Earth Environ. Sci.* **2021**, *787*, 012018. [[CrossRef](#)]
8. Bekbasarov, I.; Atenov, Y. Equations Used to Calculate Vertical Bearing Capacity of Driven Piles with Shaft Broadenings. *Period. Civ. Eng.* **2020**, *64*, 1235–1243. [[CrossRef](#)]
9. Bekbasarov, I.; Shanshabayev, N. Driving Features of Tapered-Prismatic Piles and Their Resistance to Static Loads. *Acta Montan. Slovaca* **2022**, *4*, 55–65. [[CrossRef](#)]
10. Pérez, J.A.; Reyes-Rodríguez, A.M.; Sánchez-González, E.; Ríos, J.D. Experimental and Numerical Flexural–Torsional Performance of Thin-Walled Open-Ended Steel Vertical Pile Foundations Subjected to Lateral Loads. *Buildings* **2023**, *13*, 1738. [[CrossRef](#)]
11. Bekbasarov, I.; Nikitenko, M.; Shanshabayev, N.; Atenov, Y.; Moldamuratov, Z. Tapered-prismatic pile: Driving energy consumption and bearing capacity. *News Natl. Acad. Sci. Repub. Kazakhstan Ser. Geol. Tech. Sci.* **2021**, *6*, 53–63. [[CrossRef](#)]
12. Ma, L.X.; Shi, Z.P.; Han, K.; Chang, P.F.; He, X.D. Numerical simulation study of squeezed branch piles based on post-grouting technology. *E3S Web Conf. NETID* **2021**, *292*, 01038. [[CrossRef](#)]
13. Svintsov, A.P.; Amiri, R.; Rukosueva, A.A. Construction of foundations in soils with an aquifer. *Hous. Constr.* **2019**, *9*, 31–36. [[CrossRef](#)]
14. Haroon, M.; Kvartenko, K.V. Improving the technology of constructing foundations in rammed pits and devices for its implementation. *Bull. RUDN Univ.* **2012**, *3*, 114–119.

15. Glushkov, V.E.; Glushkov, A.V. Rammed foundations in soils with a weak underlying layer. *Bull. PNIPU Constr. Archit.* **2014**, *2*, 19–26.
16. Kovalev, V.A.; Kovalev, A.S. Construction of a round hollow pile with a widened base. *Hous. Constr.* **2018**, *1–2*, 66–68.
17. Kovalev, V.A.; Kovalev, A.S. Technological schemes of the device of the driven piles in punched wells in elastic shells. *Eurasian Sci. J.* **2018**, *10*, 1–8. Available online: <https://esj.today/PDF/28SAVN318.pdf> (accessed on 4 September 2023).
18. Zotsenko, N.L.; Vinnikov, Y.L.; Babenko, V.A. Strengthening the foundations of a public building using pile pressing methods. In Proceedings of the St. Petersburg-2005: Proceedings of the International Symposium, Part 2, St. Petersburg, Russia, 13–20 July 1993; pp. 130–133.
19. Kupchikova, N.V. Methodology for deformation calculation of piles with end widening in the theory of shaping of reinforcing elements. *Eng. Constr. Bull. Casp. Reg. Sci. Tech. J.* **2015**, *2*, 32–39.
20. Kupchikova, N.V. Shape formation of the end widening of bored piles taking into account experimental-analytical and numerical research. *Eng. Constr. Bull. Casp. Sea Sci. Tech. J.* **2019**, *4*, 93–98.
21. Shao, F.; Deng, Y.; Chen, S.; Zheng, R.; Zhang, R. Field Test Study on Construction Disturbances of Driven Pile and PGP Pile. *Appl. Sci.* **2023**, *13*, 11887. [[CrossRef](#)]
22. Hoffmann, M.; Zarkiewicz, K.; Zieliński, A.; Skibicki, S.; Marchewka, Ł. Foundation Piles—A New Feature for Concrete 3D Printers. *Materials* **2021**, *14*, 2545. [[CrossRef](#)]
23. Al-Recaby, M.K. Assessing The Increase In Bearing Capacity Of Bored Piles In Sandy Soil Using Expansive Additives. *Kufa J. Eng.* **2019**, *10*, 12–28. [[CrossRef](#)]
24. Monteiro, F.F.; da Cunha, R.P.; de Aguiar, M.F.P.; Silva, C.M. Bearing Capacity Assessment Of Bored Piles Equipped With Expander Body Systems Using The Mechanics Of Unsaturated Soils. *MATEC Web Conf.* **2021**, *337*, 03011. [[CrossRef](#)]
25. RD 110-31-14-84; Recommendations for the Design and Installation of Foundations from Flat-Profile Piles. DalNIIS: Vladivostok, Russia, 1985; 35p.
26. Glukhov, V.S.; Hryanina, O.V.; Glukhova, M.V. Pile-Slab Foundation on The Combined Basis. *Bull. PNIPU Constr. Archit.* **2014**, *2*, 78–84. [[CrossRef](#)]
27. Kovalev, V.A.; Kovalev, A.S. Razrabotka tekhnicheskikh resheniy ustroystva fundamentov v uplotnennom grunte [Specification of Engineering Proposals for Foundations on Compacted Fills]. *Stroit. Nauka I Obraz. Constr. Sci. Educ.* **2017**, *7*, 1. Available online: <http://www.nsojournal.ru> (accessed on 27 August 2023).
28. GOST 25100-2020; Soils. Classification. Interstate Standard: Moscow, Russia, 2020; 41p.
29. GOST 5180-2015; Soils. Methods for Laboratory Determination of Physical Characteristics. Interstate Standard: Moscow, Russia, 2019; 20p.
30. GOST 23735-2014; Sand-Gravel Mixtures for Construction Work. Technical Specifications: Moscow, Russia, 2019; 8p.
31. GOST 8267-93; Crushed Stone and Gravel from Dense Rocks for Construction Work. Technical Specifications: Moscow, Russia, 2018; 21p.
32. GOST 5686-2020; Soils. Methods for Field Testing of Piles. Interstate Standard: Moscow, Russia, 2020; 65p.
33. SP RK EN 1997-1:2004/2011; Geotechnical Design. Part 1. General Rules. KazNIISA: Astana, Kazakhstan, 2016; 156p.
34. SP RK 5.01-103-2013; Pile Foundations. KazNIISA: Nur-Sultan, Kazakhstan, 2021; 95p.

**Disclaimer/Publisher’s Note:** The statements, opinions and data contained in all publications are solely those of the individual author(s) and contributor(s) and not of MDPI and/or the editor(s). MDPI and/or the editor(s) disclaim responsibility for any injury to people or property resulting from any ideas, methods, instructions or products referred to in the content.